Contribution from the Department of Chemistry, Memorial University of Newfoundland, St. John's, Newfoundland, Canada A1B 3X7, and Chemistry Division, National Research Council, Ottawa, Ontario, Canada K1A 0R6

Structural, Magnetic, and Electrochemical Studies on Macrocyclic Dicopper(II) Complexes with Varying Chelate Ring Size

Sanat K. Mandal,[1a] Laurence K. Thompson,*[1a] Michael J. Newlands,[1a] and Eric J. Gabe†[1b]

Received February 16, 1989

Binuclear macrocyclic copper(II) complexes involving ligands derived by condensation of 4-methyl-2,6-diacetylphenol with 1,2-diaminoethane (MeUEM) and 4-methyl-2,6-diformylphenol with 1,3-diaminopropane (UPM) and 1,4-diaminobutane (UBM), which have chelate rings of varying size (five-, six-, and seven-membered, respectively), have been compared in terms of their structural, magnetic and electrochemical properties. The binuclear center dimensions of $[Cu_2(UPM)(H_2O)_2][Cu_2(UPM)(H_2O)_2(ClO_4)_2](ClO_4)_2$ and $[Cu_2(UBM)(ClO_4)_2]$ are very similar, and both compounds exhibit comparable, strong antiferromagnetic exchange ($-2J$ = 850 (2) and 857 (6) cm^{-1}, respectively). $[Cu_2(MeUEM)(H_2O)_2](BF_4)_2$ has a much smaller binuclear center, including a reduced Cu–O–Cu bridge angle, and is less strongly coupled ($-2J$ = 689 (3) cm^{-1}). Chelate ring size also affects $E_1/_2$ values for one-electron reduction, with $[Cu_2(UBM)(ClO_4)_2]$ exhibiting the most positive reduction potentials. The crystal and molecular structures of $[Cu_2(UPM)(H_2O)_2][Cu_2(UPM)(H_2O)_2(ClO_4)_2](ClO_4)_2$ (I) and $[Cu_2(UBM)(ClO_4)_2]$ (II) are reported. I crystallized in the monoclinic system, space group $P2_1/a$, with a = 14.7242 (5) Å, b = 12.3816 (3) Å, c = 16.5571 (6) Å, β = 105.681 (3)°, and Z = 4. II crystallized in the monoclinic system, space group $P2_1/c$, with a = 8.6653 (3) Å, b = 16.7173 (13) Å, c = 9.9714 (6) Å, β = 97.273 (4)°, and Z = 8. Two different molecules are found in the unit cell of I, one involving square-pyramidal copper centers and the other six-coordinate copper centers. In II two asymmetrically bound, axial, bidentate perchlorates complete the distorted six-coordinate structure at each copper atom.

Introduction

Macrocyclic dicopper(II) complexes of Robson-type ligands have been the focus of a great deal of recent attention,[2-17] especially from the standpoint of their electrochemical properties. Sequential one-electron-reduction steps at negative potentials (V vs SCE) with large potential separations lead to the generation of relatively stable "odd"-electron intermediates that exhibit commonly four-line and less commonly seven-line EPR spectra in solution.[4,6,8,11,15] The four-line spectrum indicates the localization of the odd electron at one copper center, while the seven-line spectrum indicates delocalization of the electron over both copper centers ($I = {}^3/_2$). It is significant that seven-line spectra have only been obtained for ligands involving unsaturated nitrogen donors derived from 2,6-diformylphenols (Figure 1; R = H, R′ = Me, n = 3, 4; R = H, R′ = tBu, n = 3,4[6,8,11]) and that nitrogen saturation and substitution at the azomethine carbon center leads to four-line spectra.[4,15] Saturation of the azomethine nitrogen donors leads to macrocyclic dicopper(II) complexes that, in addition to undergoing sequential one-electron-reduction steps, can also undergo sequential one-electron oxidation with the formation of $Cu^{II}Cu^{III}$ and $Cu^{III}Cu^{III}$ species.[15] Odd-electron intermediates have been shown to exhibit four-line solution EPR spectra at room temperature.[15] The proximity of the two copper(II) centers in these phenoxo-bridged complexes leads to a situation where strong antiferromagnetic exchange has been observed,[2,7,15,17] according to variable-temperature magnetic studies, with $-2J > 580$ cm^{-1}.

In this report we describe the X-ray structures of the complexes $[Cu_2(UPM)(H_2O)_2][Cu_2(UPM)(H_2O)_2(ClO_4)_2](ClO_4)_2$ (I) and $[Cu_2(UBM)(ClO_4)_2]$ (II) (Figure 1). Both of these compounds have been reported previously, but no structural details have been published (I,[2,6,8,10,17] II[17]). Two different molecules exist in the unit cell in I, one involving square-pyramidal copper(II) centers with axially bound water and the other involving six-coordinate copper(II) centers with a trans-axial arrangement of coordinated water and monodentate perchlorate. This contrasts with the complex $Cu_2(UPM)(TCNQ)_2$ (TCNQ = 7,7′,8,8′-tetracyanoquinodimethane), which contains a single binuclear cation with square-pyramidal copper(II) centers involving an apical interaction with a TCNQ nitrogen.[16] The structure of II involves two six-coordinate copper(II) atoms in an asymmetric trans arrangement having axially bound bidentate perchlorates. Both complexes exhibit very strong antiferromagnetic exchange ($-2J$ = 850 (2) (I), 857 (6) cm^{-1} (II)), a feature common to fairly planar systems of this sort involving diphenoxo bridges. The complexes $[Cu_2(MeUPM)](ClO_4)_2$ (III) and $[Cu_2(PrUPM)](ClO_4)_2 \cdot 1.5H_2O$ (IV) are also found to be strongly coupled ($-2J$ = 835 (5) (III), 806 (9) cm^{-1} (IV)).

Electrochemical studies on II indicate a more thermodynamically favored one-electron-reduction step compared with that in I, and the one-electron-reduced species exhibits a seven-line EPR spectrum. Complex V, $[Cu_2(MeUEM)(H_2O)_2](BF_4)_2$,[13] involving a macrocyclic ligand with five-membered chelate rings (Figure 1), has a one-electron-reduction potential comparable to that of I, despite the constraints imposed by the ethylene bridge.

Experimental Section

Physical Measurements. Variable-temperature magnetic susceptibility data were obtained in the temperature range 5–300 K with an Oxford Instruments superconducting Faraday magnetic susceptibility system with a Sartorius 4432 microbalance. A main solenoid field of 1.5 T and a gradient field of 10 T m^{-1} were employed. $HgCo(NCS)_4$ was used as calibrant.

The electrochemical experiments were performed at room temperature in dimethyl sulfoxide (Me_2SO; spectroscopic grade, dried over molecular sieves) and acetonitrile (spectroscopic grade, dried over molecular sieves) under O_2-free conditions with use of a BAS CV27 Voltammograph and a Hewlett-Packard XY recorder. A three-electrode system was used (cyclic voltammetry) in which the working electrode was glassy carbon (GC) and the counter electrode platinum, with a standard calomel

* To whom correspondence should be addressed.
† This paper assigned NRCC Contribution No. 30528.

(1) (a) Memorial University of Newfoundland. (b) National Research Council.
(2) Pilkington, N. H.; Robson, R. *Aust. J. Chem.* **1970**, *23*, 2225.
(3) Okawa, H.; Kida, S. *Bull. Chem. Soc. Jpn.* **1972**, *45*, 1759.
(4) Addison, A. W. *Inorg. Nucl. Chem. Lett.* **1976**, *12*, 899.
(5) Hoskins, B. F.; McLeod, N. J.; Schaap, H. A. *Aust. J. Chem.* **1976**, *29*, 515.
(6) Gagné, R. R.; Koval, C. A.; Smith, T. J. *J. Am. Chem. Soc.* **1977**, *99*, 8367.
(7) Lambert, S. L.; Hendrickson, D. N. *Inorg. Chem.* **1979**, *18*, 2683.
(8) Gagné, R. R.; Koval, C. A.; Smith, T. J.; Cimolino, M. C. *J. Am. Chem. Soc.* **1979**, *101*, 4571.
(9) Gagné, R. R.; Henling, L. M.; Kistenmacher, T. J. *Inorg. Chem.* **1980**, *19*, 1226.
(10) Mandal, S. K.; Nag, K. *J. Chem. Soc., Dalton Trans.* **1983**, 2429.
(11) Long, R. S.; Hendrickson, D. N. *J. Am. Chem. Soc.* **1983**, *105*, 1513.
(12) Mandal, S. K.; Nag, K. *J. Chem. Soc., Dalton Trans.* **1984**, 2141.
(13) Carlisle, W. D.; Fenton, D. E.; Roberts, P. B.; Casellato, U.; Vigato, P. A.; Graziani, R. *Transition Met. Chem.* **1986**, *11*, 292.
(14) Mandal, S. K.; Thompson, L. K.; Nag, K.; Charland, J.-P.; Gabe, E. J. *Inorg. Chem.* **1987**, *26*, 1391.
(15) Mandal, S. K.; Thompson, L. K.; Nag, K.; Charland, J.-P.; Gabe, E. J. *Can. J. Chem.* **1987**, *65*, 2815.
(16) Lacroix, P.; Kahn, O.; Gleizes, A.; Valade, L.; Cassoux, P. *Nouv. J. Chim.* **1984**, *8*, 643.
(17) Lacroix, P.; Kahn, O.; Theobald, F.; Leroy, J.; Wakselman, C. *Inorg. Chim. Acta* **1988**, *142*, 129.

0020-1669/89/1328-3707$01.50/0

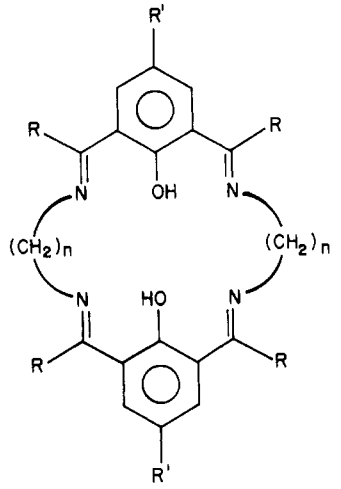

Figure 1. Macrocyclic ligands UPM (R = H, R′ = Me, n = 3), UBM (R = H, R′ = Me, n = 4), MeUPM (R = Me, R′ = Me, n = 3), PrUPM (R = Pr^n, R′ = Me, n = 3), and MeUEM (R = Me, R′ = Me, n = 2).

electrode (SCE) as reference. The ferrocenium/ferrocene internal potential marker has been used to compare redox potentials in Me_2SO, and $E_{1/2}$ values are also quoted versus the normal hydrogen electrode (NHE) ($E_{1/2}(Fc^+/Fc)$ = +0.400 V vs NHE).[18] For coulometry measurements a three-electrode system was employed consisting of a platinum-mesh-flag working electrode, a platinum-mesh counter electrode, and a SCE reference electrode. The supporting electrolyte was tetraethylammonium perchlorate (TEAP) or tetrabutylammonium perchlorate (TBAP; 0.1 M), and all solutions were 10^{-3}–10^{-4} M in complex. The best combination of experimental conditions (working electrode, scan rates, solvent, etc.) was determined by preliminary experiments.

EPR experiments were carried out at room temperature by using a Bruker ESP 300 X-band spectrometer. Samples of the air-sensitive mixed-valence species were prepared under nitrogen and loaded into the EPR tubes with use of syringe techniques.

Synthesis of Complexes. $[Cu_2(UBM)(ClO_4)_2]$ (II). 1,4-Diaminobutane (0.612 g, 6.00 mmol) dissolved in methanol (10 mL) was added to a solution of $Cu(ClO_4)_2 \cdot 6H_2O$ (1.48 g, 4.00 mmol) in methanol (25 mL). A solution of 2,6-diformyl-4-methylphenol[19] (0.654 g, 4.00 mmol) in hot methanol (50 mL) was then added and the resulting mixture refluxed for 7 h with stirring. When the mixture was cooled to room temperature, a dark khaki green microcrystalline product was obtained, which was collected by filtration and washed several times with cold water. Well-grown crystals suitable for X-ray analysis were obtained by making a boiling saturated aqueous solution of the compound and allowing it to cool slowly to room temperature (yield 1.12 g). Anal. Calcd for $[Cu_2(C_{26}H_{30}N_4O_2)(ClO_4)_2]$: C, 41.28; H, 4.00; N, 7.41. Found: C, 41.35; H, 3.94; N, 7.32. The synthesis of this compound has been reported previously.[17]

The syntheses of the complexes $[Cu_2(UPM)(H_2O)_2][Cu_2(UPM)(H_2O)_2(ClO_4)_2](ClO_4)_2$ (I),[10] $[Cu_2(MeUPM)](ClO_4)_2$ (III),[4,10] $[Cu_2(PrUPM)](ClO_4)_2 \cdot 1.5H_2O$ (IV),[10] and $[Cu_2(MeUEM)(H_2O)_2](BF_4)_2$ (V)[13] have been reported already. Anal. Calcd for $[Cu_2(C_{26}H_{30}N_4O_2)(H_2O)_2](BF_4)_2$ (V): C, 40.68; H, 4.46; N, 7.30. Found: C, 41.11; H, 4.48; N, 7.52.

Crystallographic Data Collection and Refinement of the Structures. $[Cu_2(UPM)(H_2O)_2][Cu_2(UPM)(H_2O)_2(ClO_4)_2](ClO_4)_2$ (I). Crystals of I are green. The diffraction intensities of an approximately 0.20 × 0.20 × 0.20 mm crystal were collected with graphite-monochromatized Cu Kα radiation by using the $\theta/2\theta$ scan technique with profile analysis[20] to $2\theta_{max}$ = 99.9° on a Picker four-circle diffractometer at 295 K. A total of 2999 reflections were measured, of which 2996 were unique and 2197 were considered significant with $I_{net} > 2.5\sigma(I_{net})$. Lorentz and polarization factors were applied, but no correction was made for absorption. The cell parameters were obtained by the least-squares refinement of the setting angles of 68 reflections with 2θ = 100–120° (λ(Cu Kα) = 1.540 56 Å).

The structure was solved by direct methods with use of MULTAN[21] and refined by full-matrix least-squares methods to final residuals of R = 0.061 and R_w = 0.049 for the significant data (0.088 and 0.051 for all data) with weights based on counting statistics. Hydrogen atoms were placed in calculated positions but not refined. Crystal data are given in Table I, and final atomic positional parameters and equivalent isotropic

Table I. Crystallographic Data for $[Cu_2(UPM)(H_2O)_2][Cu_2(UPM)(H_2O)_2(ClO_4)_2](ClO_4)_2$ (I) and $[Cu_2(UBM)(ClO_4)_2]$ (II)

(a) Compound I	
chem formula: $Cu_2C_{24}H_{26}Cl_2N_4O_{12}$	fw = 751.41
a = 14.7242 (5) Å	space group: $P2_1/a$
b = 12.3816 (3) Å	T = 22 °C
c = 16.5571 (6) Å	λ = 1.540 56 Å
β = 105.681 (3)°	ρ_{calcd} = 1.717 g cm^{-3}
V = 2906.17 Å^3	μ = 4.04 mm^{-1}
Z = 4	R = 0.061
	R_w = 0.049
(b) Compound II	
chem formula: $Cu_2C_{26}H_{30}Cl_2N_4O_{10}$	fw = 189.13
a = 8.6653 (3) Å	space group: $P2_1/c$
b = 16.7173 (13) Å	T = 22 °C
c = 9.9714 (6) Å	λ = 0.709 30 Å
β = 97.273 (4)°	ρ_{calcd} = 1.754 g cm^{-3}
V = 1432.84 Å^3	μ = 1.74 mm^{-1}
Z = 8	R = 0.060
	R_w = 0.063

Table II. Final Atomic Positional Parameters and Equivalent Isotropic Debye–Waller Temperature Factors (Esd's) for $[Cu_2(UPM)(H_2O)_2][Cu_2(UPM)(H_2O)_2(ClO_4)_2](ClO_4)_2$ (I)

	x	y	z	B_{iso}, Å^{2a}
Cu(1)	0.47662 (10)	0.38546 (11)	0.46311 (9)	2.97 (8)
Cl(1)	0.3197 (3)	0.05479 (25)	0.09902 (23)	4.83 (20)
Cl(2)	0.2302 (3)	0.3791 (3)	0.4891 (3)	5.85 (22)
O(1)	0.4700 (5)	0.5390 (5)	0.4284 (4)	2.8 (4)
O(3)	0.2259 (7)	0.0212 (7)	0.0642 (6)	8.6 (6)
O(4)	0.3176 (6)	0.1673 (6)	0.1082 (5)	7.3 (6)
O(5)	0.3718 (8)	0.0274 (9)	0.0463 (7)	12.8 (9)
O(6)	0.3560 (9)	0.0070 (7)	0.1761 (6)	12.0 (9)
O(7)	0.3088 (7)	0.4262 (10)	0.4765 (8)	13.3 (10)
O(8)	0.1947 (9)	0.4368 (9)	0.5422 (8)	12.7 (10)
O(9)	0.2563 (8)	0.2781 (8)	0.5219 (7)	10.9 (8)
O(10)	0.1603 (9)	0.3713 (10)	0.4177 (7)	14.2 (9)
$H_2O(1)$	0.6345 (6)	0.3830 (8)	0.4409 (5)	8.7 (7)
N(1)	0.4235 (6)	0.3366 (7)	0.3476 (5)	3.4 (5)
N(2)	0.4863 (6)	0.2435 (6)	0.5166 (5)	2.6 (5)
C(1)	0.4265 (7)	0.5839 (9)	0.3557 (6)	2.5 (6)
C(2)	0.4208 (7)	0.6957 (8)	0.3448 (7)	2.6 (6)
C(3)	0.3732 (9)	0.7355 (11)	0.2657 (9)	3.7 (8)
C(4)	0.3322 (8)	0.6752 (11)	0.1965 (7)	3.5 (7)
C(5)	0.3412 (8)	0.5673 (11)	0.2075 (7)	3.4 (7)
C(6)	0.3871 (7)	0.5172 (8)	0.2848 (6)	2.6 (6)
C(7)	0.2829 (15)	0.7282 (17)	0.1161 (11)	5.7 (11)
C(8)	0.3906 (8)	0.3997 (9)	0.2854 (7)	3.5 (6)
C(9)	0.4225 (14)	0.2211 (10)	0.3276 (10)	6.6 (11)
C(10)	0.3822 (22)	0.1626 (19)	0.3839 (14)	8.5 (15)
C(11)	0.4429 (12)	0.1433 (10)	0.4726 (10)	4.1 (8)
C(12)	0.5334 (7)	0.2257 (8)	0.5923 (7)	2.9 (6)
Cu(2)	0.03470 (11)	1.09101 (11)	0.06516 (9)	3.18 (9)
O(2)	0.0113 (4)	0.9342 (5)	0.0565 (4)	2.7 (4)
$H_2O(2)$	0.8704 (4)	0.1268 (5)	0.0632 (4)	3.7 (4)
N(3)	0.0874 (6)	1.0877 (7)	0.1861 (6)	3.9 (5)
N(4)	−0.0595 (6)	0.7538 (6)	−0.0495 (6)	3.4 (5)
C(21)	0.0398 (7)	0.8590 (8)	0.1158 (7)	2.7 (6)
C(22)	0.0239 (8)	0.7495 (8)	0.0975 (7)	2.9 (6)
C(23)	0.0563 (8)	0.6733 (10)	0.1613 (8)	3.8 (7)
C(24)	0.1047 (8)	0.6970 (9)	0.2413 (8)	3.6 (7)
C(25)	0.1174 (10)	0.8034 (12)	0.2574 (9)	4.2 (9)
C(26)	0.0883 (8)	0.8878 (9)	0.1990 (7)	3.2 (6)
C(27)	0.1392 (17)	0.6080 (17)	0.3067 (11)	7.2 (12)
C(28)	0.1031 (10)	0.9992 (12)	0.2261 (8)	4.7 (8)
C(29)	0.1165 (11)	1.1895 (10)	0.2359 (7)	6.8 (10)
C(30)	0.08446	1.28990	0.19804	3.69
C(30)′	0.15580	1.26945	0.20247	4.47
C(31)	−0.1106 (9)	0.6857 (9)	−0.1206 (8)	5.4 (8)
C(32)	−0.0277 (7)	0.7018 (9)	0.0184 (7)	3.4 (7)

[a] B_{iso} is the mean of the principal axes of the thermal ellipsoid.

(18) Koepp, H. M.; Wendt, H.; Strehlow, H. *Z. Elektrochem.* **1960**, *64*, 483.
(19) Ullman, F.; Brittner, K. *Chem. Ber.* **1909**, *42*, 2539.
(20) Grant, D. F.; Gabe, E. J. *J. Appl. Crystallogr.* **1978**, *11*, 114.
(21) Germain, G.; Main, P.; Woolfson, M. M. *Acta Crystallogr.* **1971**, *A27*, 368.

Table III. Final Atomic Positional Parameters and Equivalent Isotropic Debye–Waller Temperature Factors (Esd's) for $[Cu_2(UBM)(ClO_4)_2]$ (II)

	x	y	z	B_{iso}, Å^{2a}
Cu	0.10151 (4)	0.027441 (23)	0.39543 (4)	2.367 (13)
Cl	−0.19441 (9)	−0.10227 (5)	0.23830 (8)	3.15 (3)
O	0.09174 (23)	−0.05545 (12)	0.53067 (20)	2.45 (7)
O(1)	−0.0352 (3)	−0.07667 (19)	0.2403 (3)	4.81 (13)
O(2)	−0.2306 (4)	−0.10964 (20)	0.3738 (3)	5.37 (14)
O(3)	−0.2126 (4)	−0.17684 (18)	0.1689 (3)	5.82 (16)
O(4)	−0.2935 (4)	−0.04511 (22)	0.1662 (4)	7.02 (18)
N(1)	0.3071 (3)	−0.01062 (15)	0.35559 (25)	2.53 (10)
N(2)	0.0644 (3)	0.11283 (16)	0.26425 (24)	2.58 (10)
C(1)	0.1514 (3)	−0.12831 (18)	0.5273 (3)	2.27 (10)
C(2)	0.1074 (3)	−0.19015 (18)	0.6099 (3)	2.39 (10)
C(3)	0.1651 (3)	−0.26741 (19)	0.5986 (3)	2.68 (11)
C(4)	0.2706 (4)	−0.28644 (19)	0.5102 (3)	2.82 (12)
C(5)	0.3239 (4)	−0.22398 (20)	0.4387 (3)	2.78 (11)
C(6)	0.2680 (3)	−0.14535 (18)	0.4445 (3)	2.42 (11)
C(7)	0.3248 (6)	−0.37136 (25)	0.4968 (5)	4.30 (18)
C(8)	0.3456 (3)	−0.08432 (20)	0.3748 (3)	2.68 (12)
C(9)	0.4282 (4)	0.03776 (22)	0.2972 (4)	3.19 (14)
C(10)	0.3992 (4)	0.12700 (21)	0.2925 (3)	3.18 (13)
C(11)	0.2976 (4)	0.15458 (24)	0.1654 (3)	3.39 (14)
C(12)	0.1434 (4)	0.11067 (24)	0.1411 (3)	3.14 (13)
C(13)	−0.0136 (4)	0.17617 (21)	0.2820 (3)	2.77 (12)

[a] B_{iso} is the mean of the principal axes of the thermal ellipsoid.

temperature factors are listed in Table II. All calculations were performed with the NRCVAX system of programs,[22] and scattering factors were taken from ref 23. Anisotropic thermal parameters (Table SI) and a listing of structure factors are included as supplementary material.

$[Cu_2(UBM)(ClO_4)_2]$ (II). Crystals of II are green. The diffraction intensities of an approximately 0.20 × 0.20 × 0.20 mm crystal were collected with graphite-monochromatized Mo Kα radiation by using the $\theta/2\theta$ scan technique with profile analysis[20] to $2\theta_{max}$ = 60.0° on a Nonius diffractometer at 295 K. A total of 7023 reflections were measured, of which 4171 were unique and 2902 were considered significant with $I_{net} > 2.5\sigma(I_{net})$. Lorentz and polarization factors were applied, but no correction was made for absorption. The cell parameters were obtained by the least-squares refinement of the setting angles of 21 reflections with 2θ = 50–60° (λ(Mo Kα) = 0.709 30 Å).

The structure was solved by direct methods with use of MULTAN[21] and refined by full-matrix least-squares methods to final residuals of R = 0.060 and R_w = 0.063 for the significant data (0.089 and 0.083 for all data) with weights based on counting statistics. Hydrogen atoms were placed in calculated positions but not refined. Crystal data are given in Table I, and final atomic positional parameters and equivalent isotropic temperature factors are listed in Table III. All calculations were performed with the NRCVAX system of programs,[22] and scattering factors were taken from ref 23. Anisotropic thermal parameters (Table SII) and a listing of structure factors are included as supplementary material.

Results and Discussion

Description of the Structures of $[Cu_2(UPM)(H_2O)_2][Cu_2(UPM)(H_2O)_2(ClO_4)_2](ClO_4)_2$ (I) and $[Cu_2(UBM)(ClO_4)_2]$ (II). The structure of I is shown in Figure 2, and interatomic distances and angles relevant to the copper coordination spheres are given in Table IV. Two different molecules are found in the unit cell, one involving two pseudooctahedral copper centers with equatorial N_2O_2 donor sets provided by two azomethine nitrogen centers and two shared, phenoxide oxygen bridging atoms and bound axially by a water molecule and a monodentate perchlorate in a trans axial arrangement (Figure 2a). The axial contacts are fairly long with a copper–water distance of 2.451 (9) Å (Cu(1)–H_2O(1)) and a copper–perchlorate distance of 2.589 (10) Å (Cu(1)–O(7)). In-plane distances to the phenoxide bridge (1.981 (6), 1.989 (6) Å) are somewhat longer than those reported for related ethylenediamine- and propylenediamine-bridged complexes with weakly

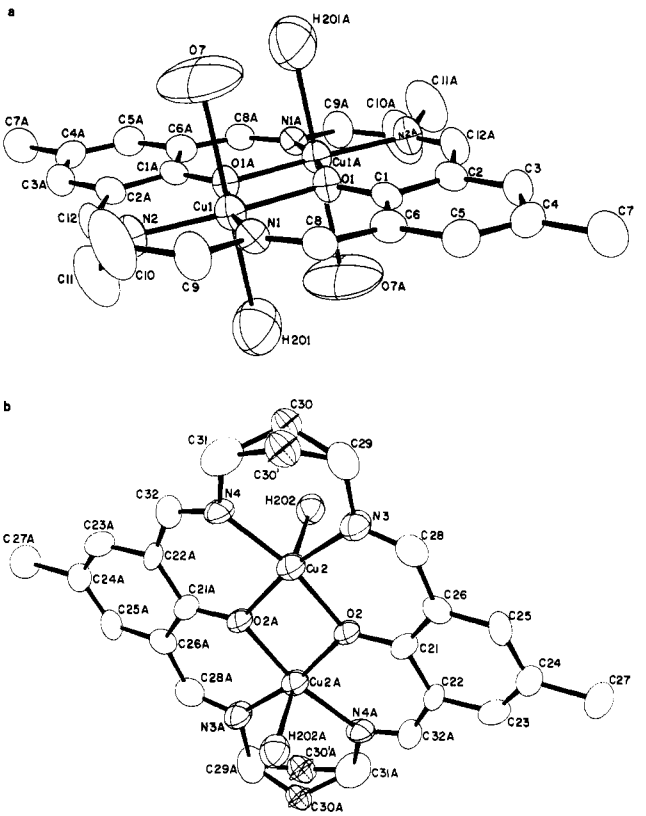

Figure 2. Structural representation for (a) $[Cu_2(UPM)(H_2O)_2(ClO_4)_2]$ of I and (b) the cation $[Cu_2(UPM)(H_2O)_2]^{2+}$ of I with hydrogen atoms omitted (40% probability thermal ellipsoids).

Table IV. Interatomic Distances (Å) and Angles (deg) Relevant to the Copper Coordination Spheres in $[Cu_2(UPM)(H_2O)_2][Cu_2(UPM)(H_2O)_2(ClO_4)_2](ClO_4)_2$ (I)

Cu(1)–Cu(1)A	3.091 (3)	Cu(1)–H_2O(1)	2.451 (9)
Cu(1)–O(1)	1.981 (6)	Cu(1)–N(1)	1.956 (8)
Cu(1)–O(1)A	1.989 (6)	Cu(1)–N(2)	1.957 (8)
Cu(1)–O(7)	2.589 (10)	O(1)–Cu(1)A	1.989 (6)
O(1)A–Cu(1)–O(7)	89.1 (3)	O(1)–Cu(1)–H_2O(1)	86.7 (3)
O(1)A–Cu(1)–H_2O(1)	89.0 (3)	O(1)–Cu(1)–N(1)	92.2 (3)
O(1)A–Cu(1)–N(1)	169.9 (3)	O(1)–Cu(1)–N(2)	170.3 (3)
O(1)A–Cu(1)–N(2)	92.9 (3)	O(7)–Cu(1)–N(2)	95.2 (4)
O(7)–Cu(1)–H_2O(1)	168.9 (4)	H_2O(1)–Cu(1)–N(1)	89.7 (3)
O(7)–Cu(1)–N(1)	90.3 (4)	H_2O(1)–Cu(1)–N(2)	95.8 (3)
O(1)–Cu(1)–O(1)A	77.7 (3)	N(1)–Cu(1)–N(2)	97.2 (4)
O(1)–Cu(1)–O(7)	82.2 (3)	Cu(1)–O(1)–Cu(1)A	102.3 (3)
Cu(2)–Cu(2)A	3.096 (3)	Cu(2)–N(3)	1.943 (9)
Cu(2)–O(2)	1.970 (6)	Cu(2)–N(4)	1.986 (8)
Cu(2)–O(2)A	1.970 (6)	O(2)–Cu(2)A	1.970 (6)
Cu(2)–H_2O(2)	2.451 (6)		
O(2)–Cu(2)–N(4)	168.1 (3)	O(2)–Cu(2)–H_2O(2)	91.42 (24)
O(2)A–Cu(2)–H_2O(2)	87.10 (24)	O(2)–Cu(2)–N(3)	93.9 (3)
O(2)A–Cu(2)–N(3)	169.3 (3)	H_2O(2)–Cu(2)–N(4)	92.2 (3)
O(2)A–Cu(2)–N(4)	92.5 (3)	N(3)–Cu(2)–N(4)	96.8 (4)
H_2O(2)–Cu(2)–N(3)	97.8 (3)	Cu(2)–O(2)–Cu(2)A	103.6 (3)
O(2)–Cu(2)–O(2)A	76.4 (3)		

coordinating or noncoordinating anions[13–15] but are the same as those reported for the trans-axial-chloro complex $[Cu_2(UPM)Cl_2]\cdot 6H_2O$.[5] Copper–nitrogen distances (1.957 (8), 1.956 (8) Å) are slightly shorter than those reported for the propylenediamine-bridged complexes[5,14,15] but longer than those reported for the ethylenediamine-bridged complex $[Cu_2(MeUEM)(H_2O)_2](BF_4)_2$ (1.90 (1), 1.92 (1) Å).[13] An oxygen bridge angle (Cu(1)–O(1)–Cu(1)A) of 102.3 (3)° is found in molecule a with a copper–copper separation of 3.091 (3) Å. The copper equatorial donor set is virtually planar with Cu(1) displaced by 0.019 (4) Å from the mean donor plane toward H_2O(1), and a slight pyramidal distortion exists at the phenoxide oxygen bridge with a solid angle of 358.4°.

(22) Gabe, E. J.; Lee, F. L.; LePage, Y. In *Crystallographic Computing III*; Sheldrick, G., Kruger, C., Goddard, R., Eds.; Clarendon Press: Oxford, England, 1985; p 167.

(23) *International Tables for X-ray Crystallography*; Kynoch Press: Birmingham, England, 1974; Vol. IV, Table 2.2B, p 99.

Table V. Interatomic Distances (Å) and Angles (deg) Relevant to the Copper Coordination Spheres in $[Cu_2(UBM)(ClO_4)_2]$ (II)

Cu–CuA	3.0354 (7)	Cu–O(2)A	2.790 (3)
Cu–O	1.9429 (20)	Cu–N(1)	1.9792 (23)
Cu–OA	1.9695 (19)	Cu–N(2)	1.935 (3)
Cu–O(1)	2.522 (3)	O(2)–CuA	2.790 (3)
O–CuA	1.9695 (19)		
O(1)–Cu–O(2)A	162.55 (9)	O–Cu–N(1)	91.69 (9)
O(1)–Cu–N(1)	91.15 (9)	O–Cu–N(2)	167.71 (9)
O(1)–Cu–N(2)	93.98 (10)	OA–Cu–O(1)	92.17 (9)
O(2)A–Cu–N(1)	92.67 (9)	OA–Cu–O(2)A	81.12 (8)
O(2)A–Cu–N(2)	102.07 (10)	OA–Cu–N(1)	168.91 (10)
N(1)–Cu–N(2)	100.26 (10)	OA–Cu–N(2)	90.07 (9)
O–Cu–OA	78.23 (8)	Cu–O–CuA	101.77 (9)
O–Cu–O(1)	82.83 (9)	Cu–O(1)–Cl	125.98 (16)
O–Cu–O(2)A	80.04 (9)	CuA–O(2)–Cl	128.57 (19)

The second molecule (Figure 2b) involves two square-pyramidal copper(II) centers bound in a manner similar to that found in molecule a, with a trans-axial arrangement of two water molecules ($Cu(2)–H_2O(2)$ = 2.451 (6) Å). The binuclear center dimensions are comparable with those found in molecule a, and the copper centers are displaced slightly (0.083 (6) Å) from the planar equatorial donor set toward $H_2O(2)$. The central carbon atom of the propane bridge (C(30)) is disordered over two positions with an occupancy of 0.4 (C(30)) and 0.6 (C(30)′). The presence of two different perchlorate groups in I is consistent with infrared data, which show three perchlorate bands around 1100 cm^{-1} (1050, 1120 cm^{-1} assigned to monodentate perchlorate and 1080 cm^{-1} assigned to ionic perchlorate).[24] The structure of this complex has not been repored previously, but the complex $[Cu_2(UPM)(TCNQ)_2]$ has been shown to contain an equivalent binuclear copper cation.[16] The dimensions at the binuclear center of this compound differ slightly from those of I (Cu–O–Cu = 104.2°, Cu–O = 1.965, 1.977 Å, Cu–N = 1.967, 1.946 Å, Cu–Cu = 3.110 Å), with the major difference involving the phenoxide bridge angle. No disorder was observed in the propylene chain. Another related complex, $[Cu_2(CF_3UPM)](ClO_4)_2$ (CF_3UPM in Figure 1; R = H, R′ = CF_3), has been shown to have a similar binuclear cation with comparable Cu–O separations and smaller phenoxide bridge angles (102.0, 101.3°), but the phenoxide oxygen atoms are displaced by 0.12 Å from the mean $N_2Cu_2N_2$ plane.[17]

The structure of II is shown in Figure 3a, and interatomic distances and angles relevant to the copper coordination spheres are given in Table V. The structure consists of a binuclear arrangement of two copper(II) centers bridged by two phenoxide oxygen atoms and each bound terminally by two azomethine nitrogen donors in the equatorial plane, with axial interactions to two perchlorate groups. Two long contacts exist to the trans-axial asymmetric bidentate perchlorates (Cu–O(1) = 2.522 (3) Å, Cu–O(2) = 2.790 (3) Å), and the copper centers are best described in terms of a distorted six-coordinate stereochemistry. A structural representation of the binuclear center in II, including the bidentate perchlorate groups, is given in Figure 3b. Such a bonding arrangement of the perchlorates is consistent with infrared data, where three perchlorate vibrations are observed (1120, 1085, 1050 cm^{-1}), indicative of a low-symmetry perchlorate.[24] The copper–copper separation (3.0354 (7) Å) and phenoxide oxygen bridge angle (101.77 (9)°) are comparable with those found in I, and the short Cu–O(1)(perchlorate) distance (2.522 (3) Å) compares closely with that found in I. The bidentate perchlorate coordination is similar to that found in the complex $[Cu_2(FPM)(ClO_4)_2]$ (FPM = UPM with all azomethine nitrogens saturated),[14] except that in this derivative the axial interactions are weaker (Cu–O = 2.821 (3) Å) and symmetric, with both copper–perchlorate oxygen distances being equal. The equatorial N_2O_2 donor set is, again, virtually planar with a slight displacement of the copper center from the mean donor plane toward the axial perchlorate oxygen, O(1), by 0.0039 (14) Å.

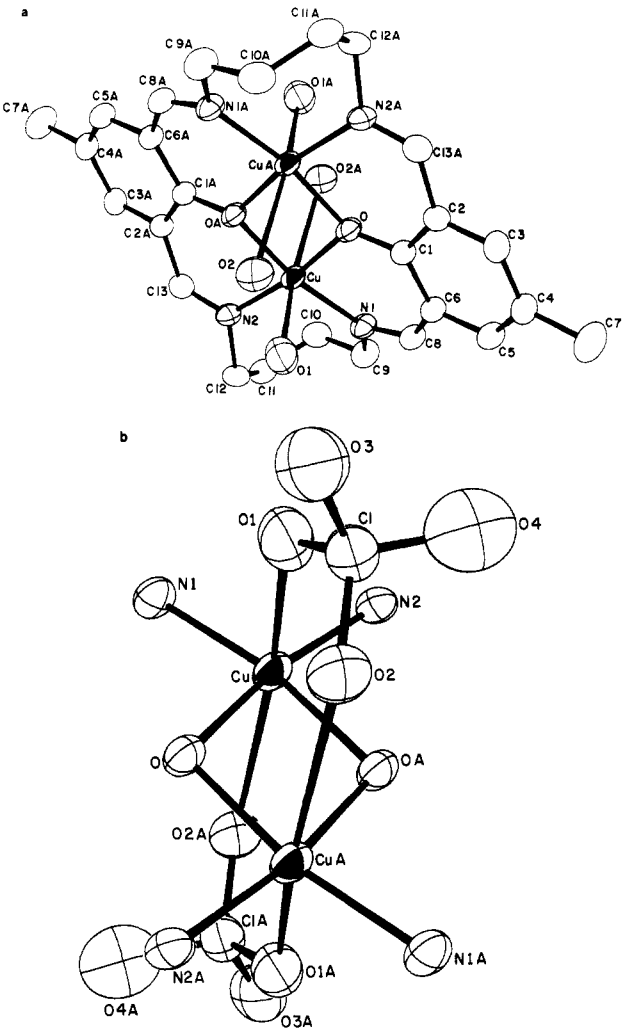

Figure 3. Structural representation for (a) $[Cu_2(UBM)(ClO_4)_2]$ (II) with hydrogen atoms omitted (40% probability thermal ellipsoids) and (b) the binuclear center in $[Cu_2(UBM)(ClO_4)_2]$ (II).

Compounds I and II involve ligands that differ only in terms of the carbon chain length between azomethine centers (three and four, respectively). Although the complex $[Cu_2(MeUEM)(H_2O)_2](BF_4)_2$ (V)[13] involves a different basic ligand with methyl substituents, rather than hydrogen, at the azomethine centers, a comparison of binuclear center dimensions of all three compounds based just on chelate ring size effects is considered to be valid. Average Cu–O and Cu–N bond lengths for V are <1.92 Å and considerably shorter than comparable bond lengths in I and II. The same is true of the copper–copper separation (2.847 (4) Å for V), phenoxide bridge angle (96.5 (5)° for V), and the angle subtended at copper by the two azomethine nitrogens[13] (92.5 (5)° (V);[13] 97.2 (4)° (Ia); 96.8 (4)° (Ib); 100.26 (10)° (II)). We have also determined the structure of V, in part to be certain that we were dealing with the same species. Our results agree with those reported previously, except that a slightly improved refinement (R = 0.087, R_w = 0.099, GOF = 1.095) has allowed a more confident appraisal of certain structural features, notably the copper–copper separation (2.997 (3) Å), the phenoxide bridge angle (98.8 (4)°), and the N–Cu–N angle (90.4 (5)°).[25] However, despite these differences, the same structural arguments apply and the smaller dimensions of the binuclear center in V can reasonably be attribued to the tight nature of the macrocycle involving the ethane bridges. The distinction between I and II is less marked and only shows up significantly when N–Cu–N angles are compared, with the bigger chelate ring in II allowing some expansion of this angle.

(24) Nakamoto, K. *Infrared and Raman Spectra of Inorganic and Coordination Compounds*, 3rd ed.; Wiley: New York, 1978.

(25) Newlands, M. J.; Gabe, E. J.; Lee, F. L. Unpublished results.

Table VI. Magnetic Data

compd	μ_{eff},[a] μ_B (T, K)	g	$-2J$, cm^{-1}	ρ[b]
$[Cu_2(UPM)(H_2O)_2][Cu_2(UPM)(H_2O)_2(ClO_4)_2](ClO_4)_2$ (I)	0.47 (298)	2.145 (11)	850 (2)	0.001
$[Cu_2(UBM)(ClO_4)_2]$ (II)	0.46 (297)	2.16 (2)	857 (6)	0.0015
$[Cu_2(MeUPM)](ClO_4)_2$ (III)	0.51 (298)	2.121 (4)	835 (5)	0.009
$[Cu_2(PrUPM)](ClO_4)_2 \cdot 1.5H_2O$ (IV)	0.58 (299)	2.154 (4)	806 (9)	0.02
$[Cu_2(MeUEM)(H_2O)_2](BF_4)_2$ (V)	0.69 (301)	2.126 (7)	689 (3)	0.006

[a] $\mu_{eff} = 2.828[(\chi_m - TIP)T]^{1/2}$. [b] Fraction of paramagnetic impurity.

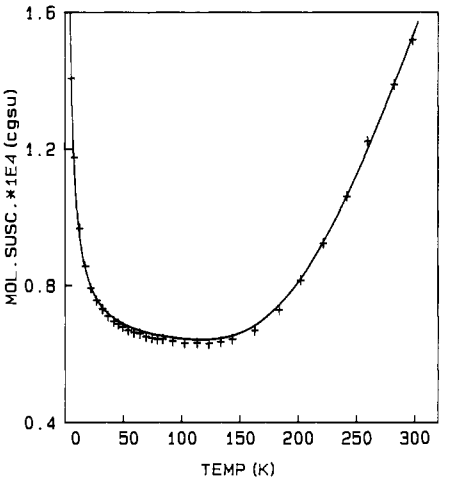

Figure 4. Average magnetic susceptibility data for $[Cu_2(UPM)(H_2O)_2][Cu_2(UPM)(H_2O)_2(ClO_4)_2](ClO_4)_2$ (I). The solid line was calculated from eq 1 with $g = 2.145$ (11), $-2J = 850$ (2) cm^{-1}, $N\alpha = 60 \times 10^{-6}$ cgsu (cm^3 mol^{-1})/Cu, and 0.1% paramagnetic impurity ($\rho = 0.0010$).

Magnetic and Electrochemical Properties. Compounds I–V all have low room-temperature magnetic moments falling in the range $\mu_{eff} = 0.45$–0.69 μ_B, indicating strong antiferromagnetic exchange between the copper centers. Variable-temperature magnetic studies have been carried out on compounds I–V in the temperature range 5–300 K, and the results are summarized in Table VI. The best-fit line in each case was calculated from the modified Van Vleck equation[26] for exchange-coupled pairs of copper(II) ions (eq 1). In this expression $2J$ (in the spin Hamiltonian $H = -2J\hat{s}_1 \cdot \hat{s}_2$) is the singlet–triplet splitting or exchange integral and other symbols have have their usual meaning (ρ represents the fraction of a possible magnetically dilute copper(II) impurity). The temperature-independent paramagnetism for a binuclear copper(II) complex, $N\alpha$, was taken as 120×10^{-6} cgsu/mol, and the parameters giving the best fit were obtained by using a nonlinear regression analysis with ρ as a floating parameter. Figure 4 illustrates the experimental molar susceptibility data, as a function of temperature, in addition to the theoretical curve for $[Cu_2(UPM)(H_2O)_2][Cu_2(UPM)(H_2O)_2(ClO_4)_2](ClO_4)_2$ (I). Similar plots were obtained for the other compounds and are included as supplementary material.

$$\chi_{M(Cu)} = \frac{N\beta^2g^2}{3kT}\left[1 + \frac{1}{3}\exp(-2J/kT)\right]^{-1}(1-\rho) + \left[\frac{N\beta^2g^2}{4kT}\right]\rho + N\alpha \quad (1)$$

Very strong net antiferromagnetic exchange is observed for compounds I–IV, with $-2J$ falling in the range 800–860 cm^{-1} (Table VI), while for compound V substantially weaker exchange is apparent. Exchange for I and II is essentially the same despite the fact that there are some significant differences in the dimensions of the Cu_2O_2 binuclear centers. The average phenoxide bridge angle in I (102.95°) is slightly larger than that in II (101.77°), the average Cu–O(bridge) distance in I is slightly larger than that in II, and the solid angle at the phenoxide bridge in I is much larger than that in II, with an angle of 353.17° in II representing a significant, but small, pyramidal distortion. Spin exchange between copper(II) centers bridged by oxygen donors (e.g. alkoxide, phenoxide) has been shown to be dependent upon the degree of pyramidal distortion at the oxygen bridge, and in severe cases the overall exchange situation can be dominated by a ferromagnetic component.[27,28] However, at this level of exchange it is clear that minor perturbations in the binuclear center dimensions do not have much of an impact on spin coupling. Even for the complex $[Cu_2(FPM)(ClO_4)_2]$, with an oxygen bridge angle of 102.8°, very short Cu–O distances (1.915 Å), and no pyramidal distortion at the phenoxide bridge, an exchange integral of $-2J = 824$ cm^{-1} was observed.[15] Compounds III and IV have slightly weaker exchange than I and II, but in the absence of any structural details it is perhaps unwise to comment on the effect of changing R (Figure 1) from hydrogen to methyl and *n*-propyl.

The variation in chelate ring size from six- to seven-membered in compounds I and II causes only minor changes in the binuclear center dimensions. However, in contrast, a somewhat compressed binuclear center exists for the five-membered chelate ring compound $[Cu_2(MeUEM)(H_2O)_2](BF_4)_2$ (V),[13,25] with a shorter metal–metal separation, shorter copper–nitrogen distances, and a smaller phenoxide bridge angle. Variable-temperature magnetic data (Table VI) indicate much weaker exchange for this compound ($-2J = 689$ (3) cm^{-1}), which can be attributed in large measure to the smaller bridge angle. These magnetic data do not agree with the reported room-temperature magnetic moment for this compound (1.44 μ_B).[13]

Variable-temperature magnetic studies have been reported recently for the compounds $[Cu_2(UPM)](ClO_4)_2 \cdot 2H_2O$ and $[Cu_2(CF_3UPM)](ClO_4)_2$ ($-2J = 712$ (10), 710 (10) cm^{-1}, respectively).[17] The difference between $[Cu_2(UPM)](ClO_4)_2 \cdot 2H_2O$ and I is surprising but may reflect the possible formation of different structural modifications of this system. Both compounds are, however, strongly antiferromagnetically coupled. A limited variable-temperature magnetic study on $[Cu_2(UPM)](ClO_4)_2 \cdot 2H_2O$ was originally reported by Robson,[2] but no analysis of the data was carried out. However, the reported room-temperature magnetic moment (0.58 μ_B (296 K)), which does not appear to have been corrected for temperature-independent paramagnetism, agrees well with our data (0.60 μ_B (298.0 K)). In another report a value of 0.60 μ_B (25 °C) was quoted for μ_{eff} of $[Cu_2(UPM)](ClO_4)_2 \cdot 2H_2O$.[8] The experimental difficulty of measuring susceptibilities for such weakly paramagnetic, spin-coupled systems may lead to discrepancies in results reported by various groups. For example, in another report, a value of 0.74 μ_B (μ_{eff} at room temperature) was quoted for this complex.[10]

There are clearly not enough data on systems of this sort, especially in terms of widely varying binuclear center dimensions, in order to assess any meaningful magnetostructural correlations. This is in contrast to the situation for bis(μ-hydroxo) complexes of the type $[Cu_2B_2(OH)_2]^{2+}$ (B = bidentate nitrogen donor), where for d_{xy}-ground-state copper centers a linear relationship exists between the exchange integral and hydroxide bridge angle[29] and

(26) Van Vleck, J. H. *The Theory of Electric and Magnetic Susceptibilities*; Oxford University Press: London, 1932; Chapter 9.

(27) Murray, K. S. In *Copper Coordination Chemistry: Inorganic and Biological Perspectives*; Karlin, K. D., Zubieta, J., Eds.; Adenine Press: New York, 1985.

(28) Mazurek, W.; Kennedy, B. J.; Murray, K. S.; O'Connor, M. J.; Rogers, J. R.; Snow, M. R.; Wedd, A. G.; Zwack, P. R. *Inorg. Chem.* **1985**, *24*, 3258.

Table VII. Electrochemical Data for the Reduction of I–V

complex	$Cu^{II}/Cu^{II} \rightarrow Cu^{II}/Cu^{I}$ (1) ΔE_p,[e] mV	$E_{1/2}$,[f] V (SCE)	$E_{1/2}$, V (NHE)	$Cu^{II}/Cu^{I} \rightarrow Cu^{I}/Cu^{I}$ (2) ΔE_p,[e] mV	$E_{1/2}$,[f] V (SCE)	$E_{1/2}$, V (NHE)	ΔE,[g] V	K_{con}[h]	ref
$[Cu_2(UPM)(H_2O)_2]$-$[Cu_2(UPM)(H_2O)_2(ClO_4)_2](ClO_4)_2$ (I)	90[a]	−0.41	−0.46	110	−0.89	−0.94	0.48	1.3×10^8	14
$[Cu_2(UBM)(ClO_4)_2]$ (II)	100[b]	−0.30	−0.35	100	−0.76	−0.81	0.46	6.0×10^7	
	90[c]	−0.24		100	−0.75		0.51	4.3×10^8	
$[Cu_2(MeUPM)](ClO_4)_2$ (III)	100[b]	−0.46	−0.52	120	−1.04	−1.10	0.58	6.5×10^9	
	60[d]	−0.46		60	−1.23		0.77	1.2×10^{13}	10
$[Cu_2(PrUPM)](ClO_4)_2 \cdot 1.5H_2O$ (IV)	90[b]	−0.45	−0.49	200	−1.00	−1.04			
	60[d]	−0.47		60	−1.25		0.78	1.6×10^{13}	10
$[Cu_2(MeUEM)(H_2O)_2](BF_4)_2$ (V)	120[a]	−0.41	−0.46	100	−1.15	−1.20	0.74	3.3×10^{12}	

[a] Me_2SO/GC/TEAP/SCE. [b] Me_2SO/GC/TBAP/SCE. [c] CH_3CN/GC/TBAP/SCE. [d] CH_3CN/HMDE/TEAP/SCE (HMDE = hanging mercury drop electrode). [e] $\Delta E_p = E_{p,c} - E_{p,a}$ at a scan rate of 200 mV s^{-1}. [f] $E_{1/2} = 0.5(E_{p,c} + E_{p,a})$. [g] $\Delta E = E_{1/2}(1) - E_{1/2}(2)$. [h] $K_{con} = \exp(nF(\Delta E)/RT)$.

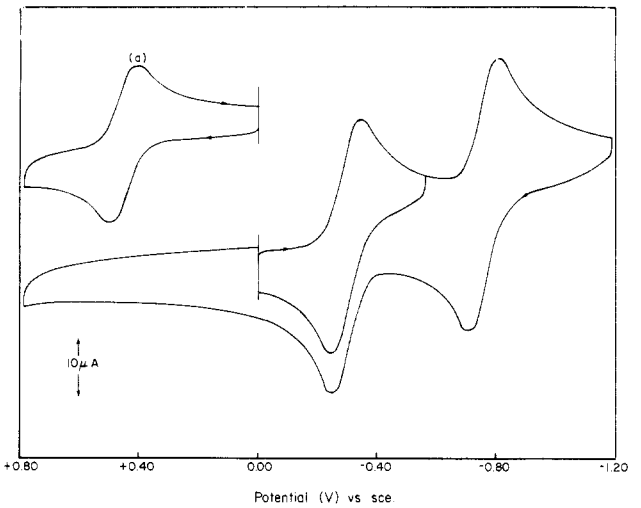

Figure 5. Cyclic voltammogram for $[Cu_2(UBM)(ClO_4)_2]$ (II) in Me_2SO (1×10^{-3} M, 0.1 M TBAP, GC electrode, SCE reference, scan rate 200 mV s^{-1}). (a) indicates the ferrocene voltammogram.

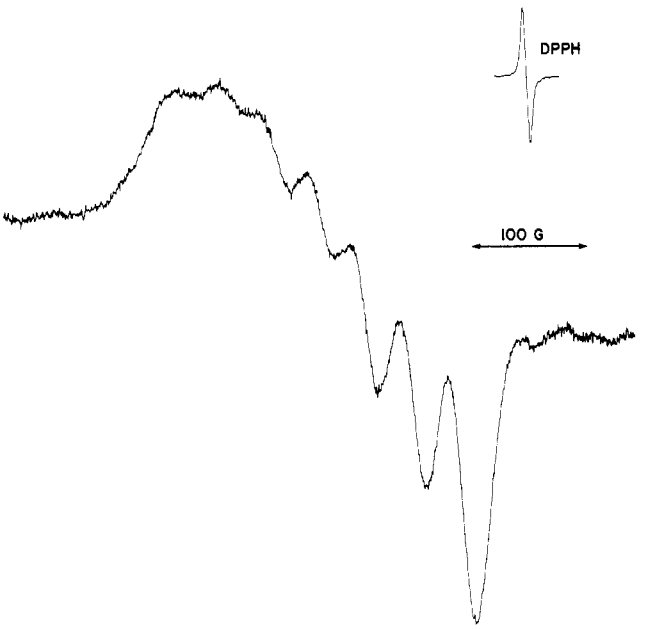

Figure 6. Room-temperature X-band EPR spectrum for one-electron-reduced species generated by coulometric reduction of $[Cu_2(UBM)(ClO_4)_2]$ (II) in CH_3CN (−0.50 V vs SCE).

for systems with bridge angles of <97.5° net ferromagnetism was observed. Within this series of compounds the relationship persists despite significant differences in in-plane Cu–O(bridge) distances (1.895–1.95 Å), indicating the primary sensitivity of exchange to the oxygen bridge angle. The effect of any pyramidal distortion at the bridging oxygen on exchange was not tested in this study. The significantly reduced phenoxide bridge angle in V is the major factor responsible for weaker antiferromagnetic exchange in this compound, and when the macrocyclic complexes are compared with bis(μ-hydroxo) compounds of the Hatfield type, it is clear that an angle closer to 90° is likely to be necessary to cause the changeover from antiferromagnetism to ferromagnetism. Testing this hypothesis will only be possible with the synthesis and structural and magnetic study of more related macrocyclic systems with widely varying phenoxide bridge angles. Synthetic and geometric limitations may, however, make this a difficult task.

The electrochemical properties of compounds I–V are similar in that they display two reduction waves (cyclic voltammetry) at negative potentials. Figure 5 illustrates cyclic voltammograms for II in Me_2SO (glassy-carbon electrode). Two clearly distinguishable redox processes are observed at $E_{1/2} = -0.30$ and −0.76 V (vs SCE) corresponding to stepwise one-electron reductions of the binuclear copper(II) complex through a Cu(II)–Cu(I) intermediate to a binuclear Cu(I) species. Controlled-potential electrolysis indicates that each wave corresponds to a one-electron step. Electrochemical data for this and the other compounds are given in Table VII. The ligands show no electrochemical response in the potential range +0.80 to −1.2 V. Electrochemical data for compound I have been reported previously in DMF[8,17] and DMSO,[14] and the slight differences in the one- and two-electron-reduction potentials are reasonably attributed to differences in solvent and working electrode. Electrochemical data for compound II, previously reported in DMF,[17] also compare closely with those in DMSO (Table VII).

A comparison of the $E_{1/2}$ values for the first one-electron-reduction steps for I–V in Me_2SO shows that the most thermodynamically favored process occurs for II, which can be rationalized in terms of the added molecular flexibility associated with the butylene bridge, which would enhance the stability of the copper(I) center. This effect has been noted previously in other solvents.[11,17] The second one-electron-reduction step for this system also occurs at the most positive potential for the group. The first one-electron-reduction potentials for I and V are the same, indicating that changing the chelate ring size from five- to six-membered does not promote the formation of the odd-electron intermediate. If reduction is accompanied by an out-of-plane distortion at one copper center, then it is reasonable to assume that a molecular twist involving the macrocyclic ligand can be accommodated by both UPM and UEM. However, an examination of the second one-electron-reduction potentials for I, II, andd V reveals the expected trend, indicating the restriction in molecular twisting that would accompany a second out-of-plane distortion based on chelate ring size. Ring substituent electronic effects associated with methyl (III) and propyl (IV) groups do not appear to influence the first one-electron-reduction process very much, but differences in $E_{1/2}$ values for the second reduction (versus that of I) indicate a possible electronic influence. In a related study that compared compounds I, III, and IV with other analogues involving differing substituents at the azomethine carbon centers

(29) Crawford, V. H.; Richardson, H. W.; Wasson, J. R.; Hodgson, D. J.; Hatfield, W. E. *Inorg. Chem.* **1976**, *15*, 2107.

in acetonitrile, a Hammett plot showed a linear relationship between Hammett σ_m values and the second reduction potential, indicating that electron density changes on the ligand are transmitted to the metal ions.[10] Replacement of the 4-methyl ring substituent by CF_3 in I and II has been shown to increase $E_{1/2}$ for both one-electron-reduction steps in DMF by 0.14–0.19 V, clearly indicating the transmission of a distant electron-withdrawing effect to the copper centers.[17]

The wide separation of the two reduction waves of all these compounds indicates significant stability for the one-electron intermediates, as is indicated by the large conproportionation constants (Table VII). The one-electron-reduced species derived from I exhibits a seven-line EPR spectrum at room temperature in both CH_2Cl_2 and CH_3CN, indicative of interaction of the odd electron with both copper centers.[6,8] Compound II produces a one-electron-reduced species in CH_3CN, which also exhibits a seven-line spectrum (Figure 6). The analogous copper tetrafluoroborate complex involving the butylene-bridged macrocyclic ligand derived from 4-*tert*-butyl-2,6-diformylphenol has also been shown to produce a one-electron-reduced species in CH_2Cl_2 or acetone, which exhibits a seven-line spectrum at room temperature.[11] This behavior contrasts with that associated with III and IV, which exhibit four-line spectra.[4,30]

Acknowledgment. We thank the Natural Sciences and Engineering Research Council of Canada for financial support for this study, including the purchase of the variable-temperature Faraday susceptometer and EPR spectrometer.

Supplementary Material Available: Tables SI and SII, listing thermal parameters for I and II, Tables SIII and SIV, listing complete bond lengths and angles for I and II, Tables SV and SVI, listing atomic positional parameters for hydrogen atoms in I and II, and Figures S1–S4, illustrating experimental and theoretical susceptibility curves as a function of temperature for II–V (15 pages); tables of calculated and observed structure factors for I and II (50 pages). Ordering information is given on any current masthead page.

(30) Mandal, S. K.; Thompson, L. K.; Nag, K. *Inorg. Chim. Acta* **1988**, *149*, 247.

Contribution from the Anorganisch-Chemisches Institut der Universität, Wilhelm-Klemm-Strasse 8, D-4400 Münster, FRG

Preparation, Structure, and Properties of Manganese Toluene-3,4-dithiolate Complexes in Different Oxidation States

Klaus Greiwe, Bernt Krebs, and Gerald Henkel*

Received August 2, 1988

Anaerobic reaction of $MnCl_2 \cdot 4H_2O$ with toluene-3,4-dithiolate (tdt^{2-}) in methanol yields $[Mn(tdt)_2]^{2-}$, which was isolated as its Ph_4P^+ salt. $[Ph_4P]_2[Mn(tdt)_2] \cdot 2MeOH$ (**1**) crystallizes in the monoclinic space group $P2_1/c$ with $a = 22.378$ (9) Å, $b = 12.102$ (4) Å, $c = 21.888$ (8) Å, $\beta = 110.48$ (3)°, and $Z = 4$. The X-ray structure of **1** was solved by direct methods and refined to R (R_w) = 0.063 (0.060) by using 5755 unique observed reflections ($I \geq 1.96\sigma(I)$). The anion $[Mn(tdt)_2]^{2-}$ features an extremely distorted tetrahedral MnS_4 coordination unit with mean Mn–S bond distances of 2.417 Å and mean S–Mn–S chelate angles of 88.87°. Controlled exposure of methanolic solutions of $[Mn(tdt)_2]^{2-}$ to air results in the immediate formation of a brown-red solution from which black crystals were isolated upon addition of Ph_4PBr. Crystals of $[Ph_4P]_2[Mn(tdt)_2][Mn(tdt)_2MeOH] \cdot 3MeOH$ (**2**) contain homoleptic ($[Mn(tdt)_2]^-$) and heteroleptic ($[Mn(tdt)_2MeOH]^-$) complexes simultaneously. **2** crystallizes in the triclinic space group $P\bar{1}$ with $a = 10.001$ (4) Å, $b = 19.447$ (8) Å, $c = 19.814$ (8) Å, $\alpha = 99.64$ (3)°, $\beta = 90.01$ (3)°, $\gamma = 104.12$ (3)°, and $Z = 2$. The X-ray structure was refined to R (R_w) = 0.041 (0.042) by using 9707 unique observed reflections ($I \geq 1.96\sigma(I)$). The two anions $[Mn(tdt)_2]^-$ and $[Mn(tdt)_2MeOH]^-$ occupy different crystallographic sites. The addition of a methanol molecule to the square-planar MS_4 unit of $[Mn(tdt)_2]^-$ extends the metal coordination to a square pyramid in $[Mn(tdt)_2MeOH]^-$. $[Mn(tdt)_2]^-$ and $[Mn(tdt)_2MeOH]^-$ exhibit mean Mn–S distances of 2.282 and 2.309 Å, respectively. The solid-state magnetic susceptibility of **1** is consistent with a Mn(II) high-spin configuration, while the magnetic data of **2** are indicative of high-spin Mn(III) centers. Spectral properties of solutions prepared from **2** conform to the existence of only one paramagnetic species in solution. The temperature-dependent positions of the isotropically shifted ^1H NMR signals between 220 and 340 K were measured. Assignment of the signals was accomplished by comparison with the analogous benzene-1,2-dithiolate complexes. Room-temperature ^1H NMR spectra for the iron/tdt^{2-} complexes are provided and compared with the spectra of the manganese compounds. Cyclic voltammetry and polarography in different solvents confirm the one-electron transfer for the Mn(II)/Mn(III) redox couple. The ΔE_p values are strongly affected by the nature of the electrode. A Pt electrode provides much larger peak separations in the CV spectra than a glassy-carbon electrode. Stronger coordinating solvents induce cathodically shifted $E_{1/2}$ potentials.

Introduction

In the last three decades there has been a great increase of knowledge in the chemistry of transition-metal–sulfur complexes. The coordination chemistry of several different classes of sulfur-containing ligands was investigated. Most interest was first attracted by 1,1-dithio[1] and 1,2-dithiolene[2] ligands. Especially, the assignment of oxidation states to the metal centers in the redox-active dithiolene type complexes has been and still is[3] a point of great interest. Later, the transition-metal–sulfur chemistry was largely influenced by bioinorganic aspects. To synthesize model compounds for active centers in nonheme iron–sulfur proteins and to mimic the ligation properties of cysteinyl residues in proteins were the most stimulating impetuses for the rapidly evolving thiolate (RS^-) chemistry.[4] Due to this biochemical background[5] most work was first done on iron–sulfide–thiolate clusters and iron–thiolate complexes[6] followed by the rapid exploration of the

(1) Coucouvanis, D. *Prog. Inorg. Chem.* **1970**, *11*, 233; **1979**, *26*, 301.
(2) (a) Typical 1,2-dithiolene ligands include benzene-1,2-dithiolate (bdt^{2-}), toluene-3,4-dithiolate (tdt^{2-}), tetrachlorobenzene-1,2-dithiolate ($S_2C_6Cl_4^{2-}$), 1,2-dimethylbenzene-4,5-dithiolate (xdt^{2-}), *cis*-ethylene-1,2-dithiolate ($endt^{2-}$), maleonitriledithiolate (mnt^{2-}), and bis(methoxycarbonyl)ethene-1,2-dithiolate. (b) McCleverty, J. A. *Prog. Inorg. Chem.* **1968**, *10*, 49. (c) Schrauzer, G. N. *Acc. Chem. Res.* **1969**, *2*, 72. (d) Eisenberg, R. *Prog. Inorg. Chem.* **1970**, *12*, 295. (e) Hoyer, E.; Dietzsch, W.; Schroth, W. *Z. Chem.* **1971**, *11*, 41. (f) Burns, R. P.; McAuliffe, C. A. *Adv. Inorg. Chem. Radiochem.* **1979**, *22*, 303. (g) Ibers, J. A.; Pace, L. J.; Martinsen, J.; Hoffman, B. M. *Struct. Bonding (Berlin)* **1982**, *50*, 1.
(3) Sawyer, D. T.; Srivatsa, G. S.; Bodini, M. E.; Schaefer, W. P.; Wing, R. M. *J. Am. Chem. Soc.* **1986**, *108*, 936.
(4) Dance, I. G. *Polyhedron* **1986**, *5*, 1037.
(5) (a) Beinert, H.; Thompson, A. J. *Arch. Biochem. Biophys.* **1983**, *222*, 333. (b) Lovenberg, W., Ed. *Iron-Sulfur Proteins*; Academic Press: New York, 1973, 1977; Vols. I–III. (c) Spiro, T. G., Ed. *Iron-Sulfur Proteins*; Wiley: New York, 1982.

0020-1669/89/1328-3713$01.50/0